Carrier-Based Space-Vector Coordinate-Shifted DPWM Strategy for Three-Level T-type NPC Inverters in Electric Aircraft Propulsion Applications

Feng Guo*†, Zhuxuan Ma*, Fei Diao*, Hui Cao*, Yue Zhao*
*Department of Electrical Engineering, University of Arkansas, Fayetteville, AR, 72701, USA
†Department of Electrical Engineering, University of Wisconsin-Milwaukee, Milwaukee, WI, 53201, USA
Emails: fengg@uark.edu, yuezhao@uark.edu

***Abstract*—In this paper, a new carrier-based space-vector coordinate-shifted discontinuous PWM (DPWM) strategy is proposed for three-level T-type neutral-point-clamped (3L-TNPC) inverters in integrated electric propulsion applications. For a commercial aircraft, the cruising stage usually dominates the longest in the typical mission profile, which delivers lower-rated power and therefore requires high-efficiency electric propulsion. In addition, the performance of the 3L propulsion drives highly depends on the premise of neutral-point (NP) voltage balance. Meanwhile, the computational efficiency is highly required when executing advanced modulation algorithms, particularly for adopting multilevel topologies. To leverage the aforesaid advantages at the same time, in this work, by adopting coordinate-derived modulation signals in shifted hexagons, not only can the NP voltage deviation be restored, but also reduced switching losses are achieved attributed to discontinuous pulse patterns.**

Index Terms*—Turboelectric aircraft powertrains, coordinate-shifted, discontinuous three-level modulation waves, neutral-point voltage balance, switching loss reduction.

I. Introduction

Due to net-zero carbon emissions, electrified airborne transportation is getting much more attentions in recent years, where power electronics converters become a significant momentum to deliver and distribute onboard energy in a highly efficient way [1]. To seek electric thrust in aircraft, the multilevel inverters interfacing between the electric power system (EPS) and high-speed motors play a pivotal role for the next-generation green propulsion drives, as referred to [2]-[5]. It converts a medium-voltage (MV) dc into a variable ac with less distortion, thus feeding electric machines. To pursue more penetration of electrical systems, it is feasible to embed electric starter/generator (ESG) units in turboelectric propulsion drives. Therefore, aircraft turbofan engines can be activated in a green solution before generating electric power to drive propulsion motors. Fig.1 shows the turboelectric distributed propulsion (TeDP) system studied in this work. It is noted that a bipolar structure with $\pm$ 0.5 kV is chosen as it fits all onboard loads simultaneously. In the point of view of improved output power quality, reduced dv/dt and suppressed electromagnetic interference (EMI) emissions while using the minimum switch

This work was supported in part by the U.S. National Science Foundation (NSF) under CAREER Award ECCS-1751506 and also the NSF EPSCoR RII Track-2 Program under the grant number OIA-2119691. The findings and opinions expressed in this article are those of the authors only and do not necessarily reflect the views of the sponsors.

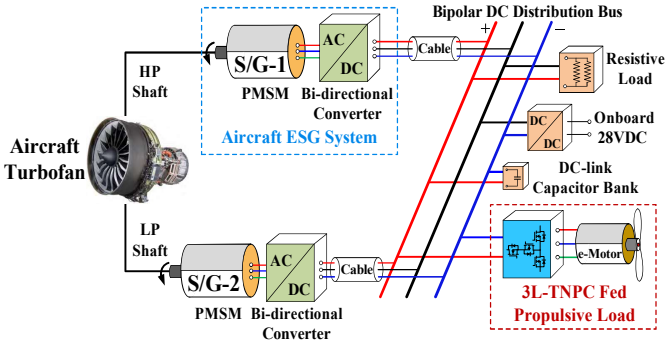

Fig. 1: The bipolar aircraft TeDP architecture.

counts for the target application, rather than other multilevel topologies, such as cascaded H-bridge (CHB) [6], active NPC (ANPC) [7] and modular multilevel converter (MMC) [8], a three-level T-type inverter shown in Fig.2 is prototyped, where the silicon-carbide (SiC) switch is selected owing to its high blocking voltage, high temperature resistance, low switching loss compared with silicon (Si) counterpart. A high-speed electric propulsion motor is fed by the high-power T-type inverter, featuring a fundamental frequency of up to a kilohertz. The overall control block diagram for the studied aircraft TeDP system can be seen in Fig.3. It incorporates machine speed control that regulates the speed of propellers, flux-weakening control that extends inverter output capability, inner-loop current control that ensures sinusoidal ac variables, droop control that adjusts the voltage level on ESP and the PWM modulator that forms the main object of this work.

However, one of the disadvantages of NPC topology is the inherent NP potential deviation due to the split dc-link capacitors, which overstresses the semiconductors and distorts the output ac variables. To address this problem without any hardware-level efforts, the PWM strategy has been explored extensively by researchers in the past years. On the one hand, the space-vector modulation (SVM) scheme paves the way for numerous balanced NP voltage variants [9]-[11], even suppressing common-mode voltage [12]-[14] and lowering switching losses [15], [16]. On the other hand, the carrier-based PWM (CBPWM) strategy can also achieve the above benefits through zero-sequence voltages (ZSVs) injection [17]-[19]. Nevertheless, it is worth noting that the SVM scheme is complicated due to the required switching sequence and dwell time determination, especially for higher output voltage

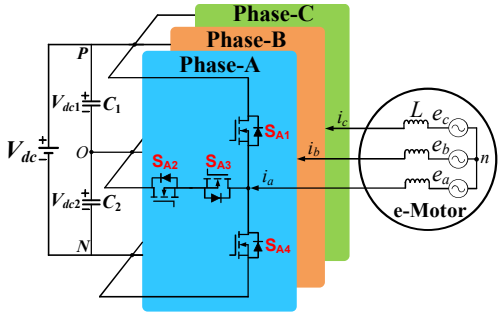

Fig. 2: The schematic of 3L-TNPC inverter-fed propulsion motor.

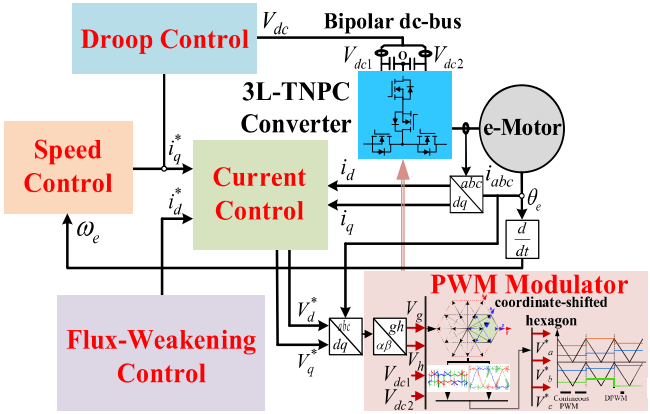

Fig. 3: Control blocks of the TeDP system.

levels. Besides, though the CB implementation is easier to attain equivalent modulation performance, an appropriate ZSV is sometimes difficult to calculate and also lacks a degree of freedom to map SV's position over a carrier period [11].

This paper proposes a new carrier-based space-vector coordinate-shifted DPWM strategy for 3L-TNPC inverters applied in the aircraft TeDP system during the cruise. By shifting the sextant coordinate of the reference SV, an order-reduced hexagon is employed to derive the relationship between two-level (2L) coordinates and modulation signals. Discontinuous pulse trains activated during the cruise are generated if fixing coordinate-based modulation waves on the top or bottom over a carrier period, resulting in fewer switching actions. Capacitor voltage balancing control by the presented PWM technique is realized by supplementing a feedback coefficient to modulation waves that reflect NP potential rise or fall. Finally, the simulation and experimental results verify the correctness and feasibility of the proposed PWM technique.

II. The Conventional SVM Strategy for 3L-TNPC Inverter

The schematic of the 3L-TNPC inverter is illustrated in Fig.2. Each phase leg of this topology consists of four switches, i.e., S_{x1}~S_{x4}, x={A, B or C}, including a half-bridge (HB) and a common-source (CS) module. in which phase x denotes phase-A, B or C. Two identical capacitors are series-connected to form the dc-bus, i.e., C_1 and C_2.

There are 27 switching states in total produced by [P], [O] and [N] by three phase legs. $+V_{dc}$ refers to S_{x1} and S_{x2} are

TABLE I: Switching Principle of 3L-TNPC Inverter

Switching States	Gating Signals (S_{x1}, S_{x2})	Output Voltages
[P]	(1, 1)	$V_{dc}/2$
[O]	(0, 1)	0
[N]	(0, 0)	$-V_{dc}/2$

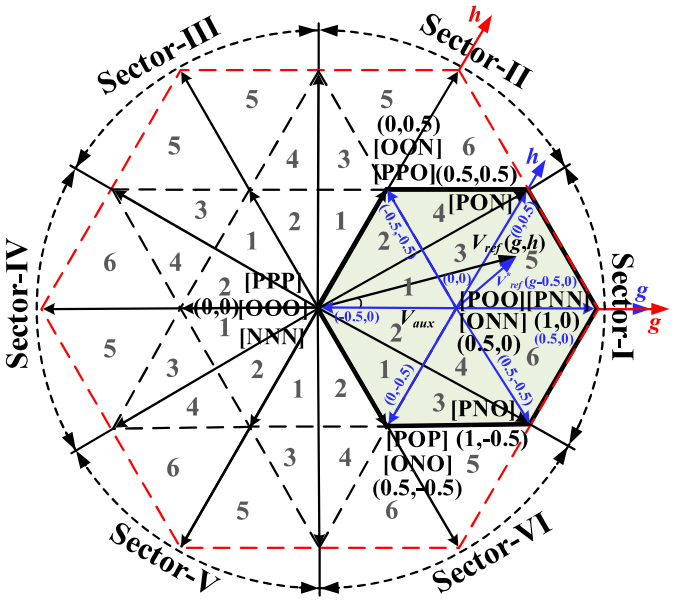

Fig. 4: Space-vector coordinate-shifted SVD.

ON, null voltage output mean that S_{x2} and S_{x3} are ON, and $-V_{dc}$ indicates that S_{x3} and S_{x4} are ON. Table I summarizes the aforesaid switching principle. The traditional SVM is also known as the seven-segment PWM.

The specific SV diagram (SVD) is given in Fig.4, but it should be pointed out that numerous switching states and dwell time calculations bring heavy computational burdens. The NP potential drifts away severely under high modulation index (MI) and low power factor (PF) conditions if a dedicated NP potential control method is not involved [10]. Though the switching actions of this method are not as many as that of the virtual SVM method [14], further reduction is desirable for lowering losses in switches, thus improving the electric propulsive efficiency at large.

III. Proposed DPWM Strategy with Space-Vector Coordinate-Shifted Modulation Waves

To streamline the conventional SVM modulation process, the equivalent modulation signals are analytically derived by a shifted 2L hexagon so that sextant coordinate-based dwell times can be deduced. For example, within an SV angle position of $\pm 30°$, as shown in Fig.4, the 3L sextant coordinates in subsector-5 of the first sextant yielded by (1) are shifted to a 2L counterpart through the corresponding new sextant plane in a smaller hexagon [20].

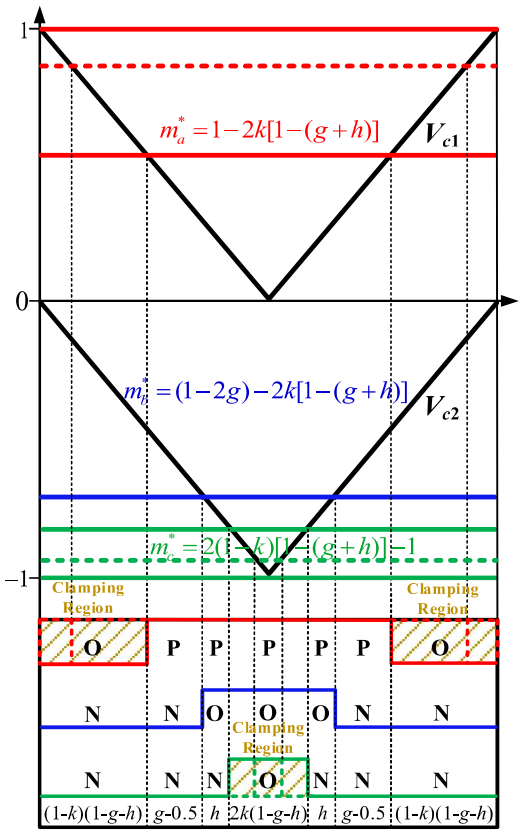

Fig. 5: CB implementation of the proposed modulation technique over a switching period.

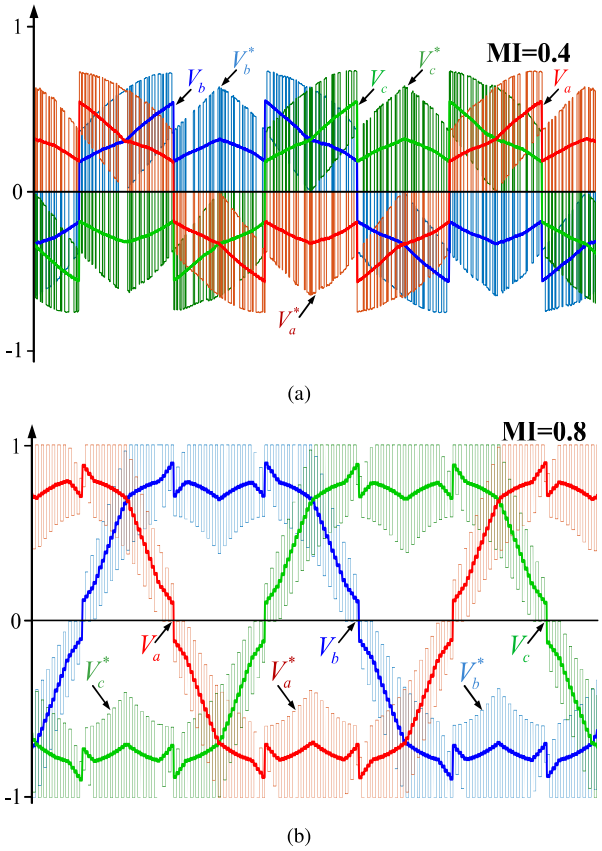

(a)

(b)

Fig. 6: Modulation waves of the proposed PWM strategy at: (a) MI=0.4. (b) MI=0.8.

$$\begin{bmatrix} V_g \\ V_h \end{bmatrix} = \begin{bmatrix} 1 & -1/\sqrt{3} \\ 0 & 2/\sqrt{3} \end{bmatrix} \begin{bmatrix} V_\alpha \\ V_\beta \end{bmatrix} \tag{1}$$

In the light of the SV composition principle, the 3L sextant coordinate-based reference SV can be determined by a 2L counterpart. After that, the basic SV coordinates labeled with blue, here is V_{aux}, are employed to calculate the dwell times of V_{ref}^* (g–0.5, 0), thus simplifying the PWM scheme effectively.

Based on the above results, modulation waves are derived from the dedicated switching patterns. For the discontinuous pulse train production, as presented in Fig.5, the modulation waves except for the middle one are fixed at the top and bottom over a carrier to gain phase clamping regions. With the equivalent P- or N-type small vector's impact on NP voltage, a factor k indicating capacitor voltages is added, accordingly. Using similar triangles, three-phase modulation signals under the continuous mode, denoted by V_a, V_b and V_c, can be updated as follows:

$$\begin{cases} V_a^* = 1-2k[1-(g+h)] \\ V_b^* = (1-2g)-2k[1-(g+h)] \\ V_c^* = 2(1-k)[1-(g+h)]-1 \end{cases} \tag{2}$$

The resultant three-phase discontinuous modulation signals derived by 2L SVM coordinates under a MI of 0.4 and 0.8 are displayed in Fig.6(a) and Fig.6(b), respectively. To assess the capacitor voltage balancing ability by this PWM algorithm,

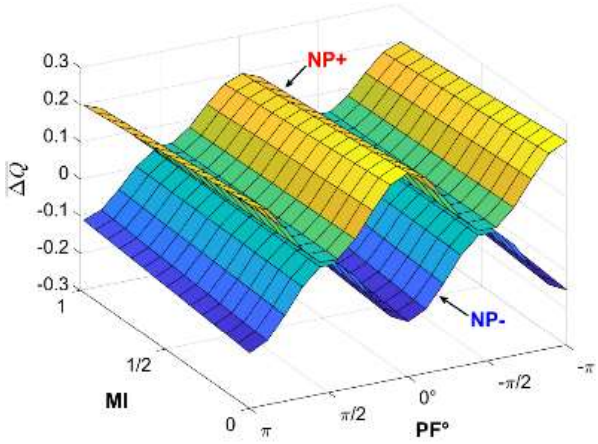

Fig. 7: Dual-polarity NP potential charges at various MIs and PFs.

Fig.7 plots available electric charges for raising (NP^+) and falling (NP^-) NP potential under various load conditions.

IV. Simulation and Experimental Results

The developed 1000 kVA aircraft TeDP system adopting a SiC-based 3L-TNPC inverter presented in Fig.2 is built in MATLAB/PLECS, and the parameters can be found in Table II. A laboratory-built and scaled-down T-type inverter-fed RL load is tested before a high-speed electric motor is available. Cree/Wolfspeed HT-3000 series 900 V power

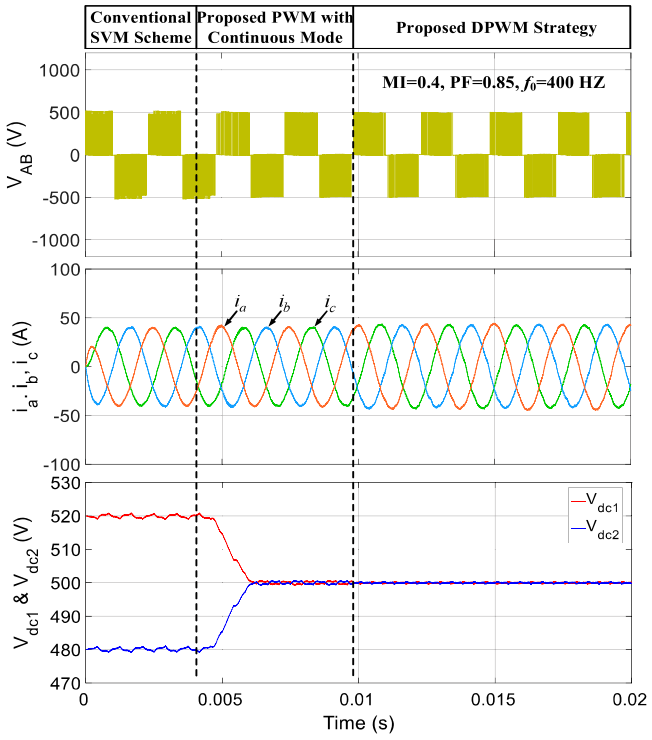

(a)

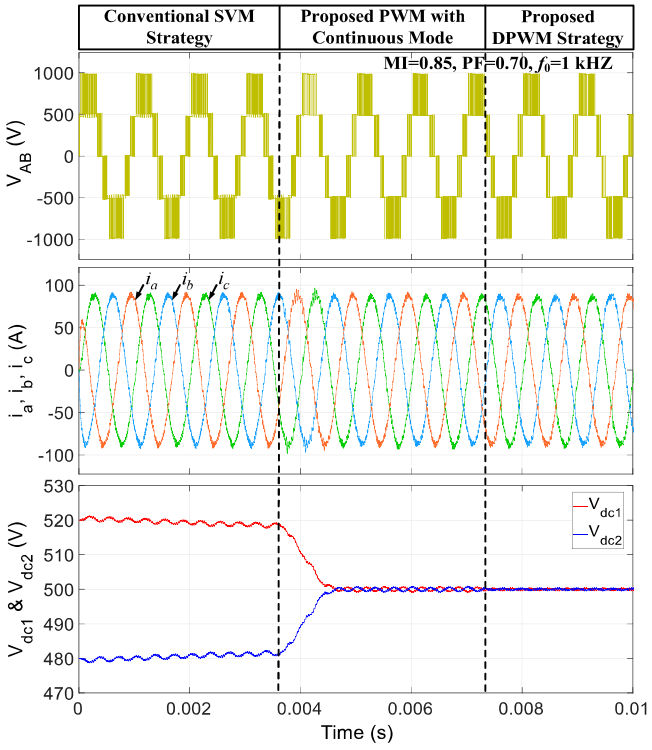

(b)

Fig. 8: 3L-TNPC inverter's output variables in the TeDP system during: (a) Startup process. (b) Cruising stage.

module is chosen to configure the circuit-level setup and its specifications are used to analyze the thermal issue produced by PWM methods in the following.

TABLE II: Parameters of Designed Aircraft TeDP System

Parameters	Simulation	Experimentation
Rated power	1000 kVA	200 kVA
DC-bus voltage	$\pm$ 540 V	$\pm$ 270 V
Switching frequency	30 kHz	30 kHz
Fundamental frequency (f_0)	$\leq$ 1 kHz	$\leq$ 1 kHz
Capacitance (C_1=C_2)	300 μF	900 μF
Modulation index (MI)	$\leq$ 0.95	$\leq$ 0.95
Power factor (PF)	0.7$\sim$1.0	0.7$\sim$1.0

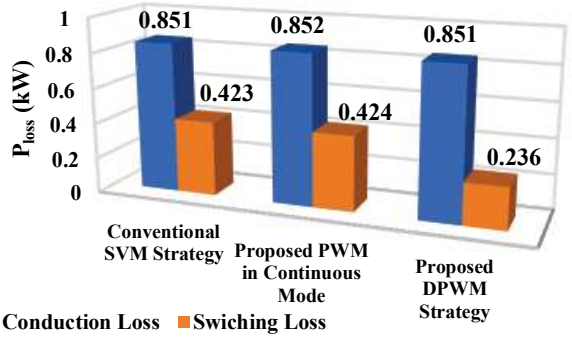

Fig. 9: The power losses breakdown.

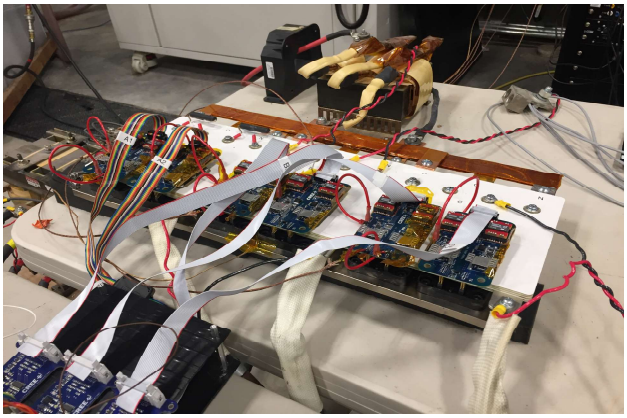

Fig. 10: All SiC-based 3L-TNPC test bench.

Fig.8 shows the 3L-TNPC inverter's output variables under different scenarios of the studied aircraft propulsion drive systems. As can be seen, the proposed PWM, not only in its continuous mode but also in the dedicated discontinuous mode (i.e., by the DPWM) for the long-range cruise, can rectify the NP voltage deviation. By using the data curves provided in the manual of the adopted semiconductors, the power loss can be analyzed through the thermal model in PLECS. Fig.9 shows the resultant power loss comparison among different modulation strategies when the output power of the TeDP system is the half of rated-power scenario. It can be seen that the continuous mode of the proposed modulation technique attains a similar loss map compared with the traditional SVM strategy, but the proposed DPWM scheme lowers the switching loss thanks to the constant pole voltage clamping regions.

The 3L-TNPC prototype is shown in Fig.10. Fig.11(a) gives the steady-state results with two balanced capacitor voltages, five-level line voltages and Phase-A current with a THD of

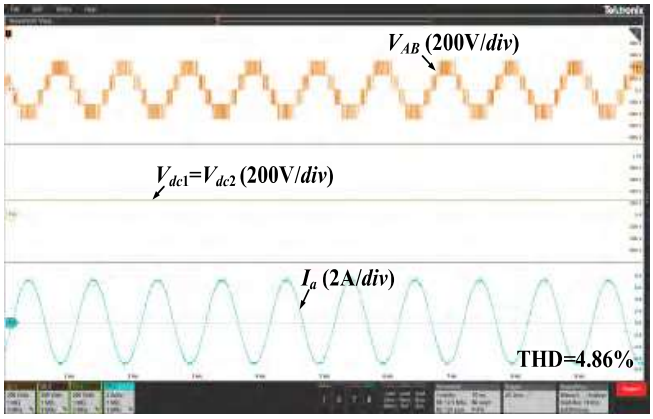

(a)

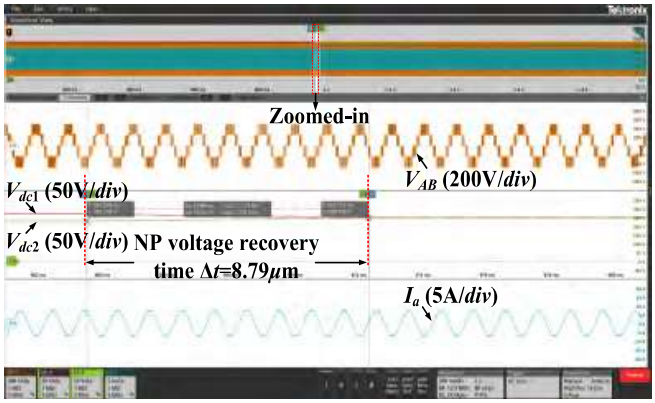

(b)

Fig. 11: The modulation performance at (a) Steady-state stage. (b) NP voltage balancing.

4.86%. Fig.11(b) shows the dynamic process of NP voltage balancing at a fundamental frequency (f_0) of 1 kHz, a MI of 0.9 and a PF of 0.75, denoting the high-speed propulsion of the TeDP system, if an initial 36 V error exists between upper and lower capacitors. As shown, only 8.79ms is required to recover the NP potential drift.

The execution time of the introduced implementation method and the original one is tested by the used digital controller, which shows an improvement of the computational efficiency of 25% with 15.2μs.

V. Conclusion

This paper proposes a novel carrier-based space-vector coordinate-shifted DPWM scheme for all SiC-based T-type 3L electric aircraft propulsion systems. The main target aims to realize NP voltage balance and lower switching loss at the cruise since it takes up most of time according to the mission profile. In order to simplify the discontinuous pulse pattern generation process, a reduced-order space-vector hexagon, that is 2L, is used to model the coordinate-driven modulation strategy. A straightforward feedback control on NP voltage is also considered in the presented approach. The simulation and experimental results verify the validate of the proposed PWM technique for the target application.

References

[1] M. T. Fard *et al.*, "Aircraft distributed electric propulsion technologies—a review," *IEEE Trans. Transp. Electrific.*, vol. 8, no. 4, pp. 4067-4090, Dec. 2022.

[2] D. Zhang, J. He and D. Pan, "A megawatt-scale medium-voltage high-efficiency high power density "SiC+Si" hybrid three-level ANPC inverter for aircraft hybrid-electric propulsion systems," *IEEE Trans. Ind. Appl.*, vol. 55, no. 6, pp. 5971-5980, Nov.-Dec. 2019.

[3] F. Guo, Z. Ma, F. Diao, Y. Zhao and P. Wheeler, "Hybrid virtual coordinate-driven CBPWM strategy of three-level T-type NPC converters for electric aircraft propulsion applications," *IEEE Trans. Ind. Electron.*, vol. 71, no. 3, pp. 2309-2319, Mar. 2024.

[4] F. Diao *et al.*, "A megawatt-scale Si/SiC hybrid multilevel inverter for electric aircraft propulsion applications," *IEEE J. Emerg. Sel. Topics Power Electron.*, vol. 11, no. 4, pp. 4095-4107, Aug. 2023.

[5] D. Wang *et al.*, "Multilevel inverters for electric aircraft applications: current status and future trends," *IEEE Trans. Transp. Electrific.*, doi: 10.1109/TTE.2023.3296284.

[6] Z. Du, B. Ozpineci, L. M. Tolbert and J. N. Chiasson, "DC–AC cascaded H-bridge multilevel boost inverter with no inductors for electric/hybrid electric vehicle applications," *IEEE Trans. Ind. Appl.*, vol. 45, no. 3, pp. 963-970, May-June, 2009.

[7] D. Pan, D. Zhang, J. He, C. Immer and M. E. Dame, "Control of MW-scale high-frequency "SiC+Si" multilevel ANPC inverter in pump-back test for aircraft hybrid-electric propulsion applications," *IEEE J. Emerg. Sel. Topics Power Electron.*, vol. 9, no. 1, pp. 1002-1012, Feb. 2021.

[8] J. Pan *et al.*, "7-kV 1-MVA SiC-based modular multilevel converter prototype for medium-voltage electric machine drives," *IEEE J. Emerg. Sel. Topics Power Electron.*, vol. 35, no. 10, pp. 10137-10149, Oct. 2020,

[9] A. Zorig, S. Barkat and A. Sangwongwanich, "Neutral point voltage balancing control based on adjusting application times of redundant vectors for three-level NPC inverter," *IEEE J. Emerg. Sel. Topics Power Electron.*, vol. 10, no. 5, pp. 5604-5613, Oct. 2022.

[10] F. Guo, T. Yang, C. Li, S. Bozhko and P. Wheeler, "Active modulation strategy for capacitor voltage balancing of three-level neutral-point-clamped converters in high-speed drives," *IEEE Trans. Ind. Electron.*, vol. 69, no. 3, pp. 2276-2287, Mar. 2022.

[11] F. Guo *et al.*, "Hybrid active modulation strategy for three-level neutral-point-clamped converters in high-speed aerospace drives," *IEEE Trans. Ind. Electron.*, vol. 70, no. 4, pp. 3449-3460, Apr. 2023.

[12] J. -H. Jung, S. -I. Hwang and J. -M. Kim, "A common-mode voltage reduction method using an active power filter for a three-phase three-level NPC PWM converter," *IEEE Trans. Ind. Appl.*, vol. 57, no. 4, pp. 3787-3800, Jul.-Aug. 2021.

[13] X. Xu, Z. Zheng, K. Wang, B. Yang and Y. Li, "A comprehensive study of common mode voltage reduction and neutral point potential balance for a back-to-back three-level NPC converter," *IEEE Trans. Power Electron.*, vol. 35, no. 8, pp. 7910-7920, Aug. 2020.

[14] F. Guo, T. Yang, A. M. Diab, S. S. Yeoh, S. Bozhko and P. Wheeler, "An enhanced virtual space vector modulation scheme of three-level NPC converters for more-electric-aircraft applications," *IEEE Trans. Ind. Appl.*, vol. 57, no. 5, pp. 5239-5251, Sept.-Oct. 2021.

[15] Y. Jiao and F. C. Lee, "New modulation scheme for three-level active neutral-point-clamped converter with loss and stress reduction," *IEEE Trans. Ind. Electron.*, vol. 62, no. 9, pp. 5468-5479, Sept. 2015.

[16] F. Guo, Z. Ma, F. Diao, Y. Zhao, P. Wheeler and Y. Cao, "Hybrid active PWM strategy with dual-mode modulation waves of three-level T-type converter for aircraft turboelectric propulsion systems," *IEEE Trans. Ind. Appl.*, doi: 10.1109/TIA.2023.3300265.

[17] F. Chen, W. Qiao, H. Wang and L. Qu, "A simple zero-sequence voltage injection method for carrier-based pulsewidth modulation of the three-level NPC Inverter," *IEEE J. Emerg. Sel. Topics Power Electron.*, vol. 9, no. 4, pp. 4687-4699, Aug. 2021.

[18] I. M. Alsofyani and K. -B. Lee, "Simple capacitor voltage balancing for three-level NPC inverter using discontinuous PWM method with hysteresis neutral-point error band," *IEEE Trans. Power Electron.*, vol. 36, no. 11, pp. 12490-12503, Nov. 2021.

[19] P. Zhang *et al.*, "A zero-sequence component injection PWM scheme for three-level neutral point clamped rectifiers with unbalanced dc-link voltages," *IEEE Trans. Ind. Electron.*, doi: 10.1109/TIE.2023.3292875.

[20] D. G. Holmes and T. A. Lipo, "Pulse width modulation for power converters – principle and practice," *Wiley-IEEE Press*, 2003.